Degradation of dye wastewater by persulfate activated with Fe$_3$O$_4$/graphene nanocomposite

Xiao-Bao Gong

ABSTRACT

In this study, Fe$_3$O$_4$/graphene nanocomposite was synthesized through a liquid-phase co-precipitation method and characterized using X-ray diffraction and Fourier transform infrared spectrometer. The synthetic Fe$_3$O$_4$/graphene was used as a heterogeneous catalyst to activate persulfate to efficiently degrade methylene blue (MB). The target pollutant MB can be degraded by sulfate radicals depending on several parameters including persulfate and Fe$_3$O$_4$/graphene concentrations, pH and reaction temperature. Within 120 min of reaction time, almost 100% of 0.05 mM MB was removed by 1.5 mM persulfate in the presence of 150 mg/L of Fe$_3$O$_4$/graphene at pH = 6.0 and 25 °C. The degradation of MB was found to follow the pseudo-first-order kinetic model. The Fe$_3$O$_4$/graphene has much better stability and reusability than free Fe$_3$O$_4$ suggested by reuse tests. The results demonstrate that Fe$_3$O$_4$/graphene activated persulfate is a promising technology for remediation of water pollution caused by organic contaminants.

Key words | magnetic nanoparticles, methylene blue, persulfate, reuse, sulfate radicals
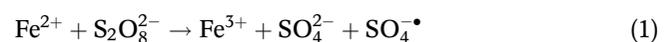
Xiao-Bao Gong
School of Civil Engineering and Architecture,
East China Jiaotong University,
Nanchang 330013,
Jiangxi,
China
E-mail: gxb@ecjtu.edu.cn

INTRODUCTION

In the last decade, advanced oxidation methods based on sulfate radicals (SO$_4^{-\bullet}$, $E^0 = 2.6$ V) have drawn considerable interest on account of the disposal of hazardous compounds in aqueous phase or soil due to its advantages, such as stability, simple operation, high efficiency and no secondary pollution (Tsitonaki et al. 2010).
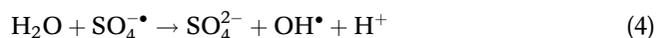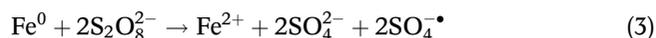
Persulfate (S$_2$O$_8^{2-}$) is one of the most common and strong oxidants ($E^0 = 2.01$ V), which can be effectively converted into sulfate radicals by the activation of heat, UV radiation, transition metal ions, zero valent metals, bimetallic and trimetallic systems (Zhang et al. 2015). Among them, the transition metal ions-induced activation of S$_2$O$_8^{2-}$ has been intensively studied and applied for the oxidation of recalcitrant organic pollutants because of its low energy consumption and cost-effectiveness (Anipsitakis & Dionysiou 2004; Chan & Chu 2009; Liu et al. 2012). Among the transition metal ions' activators, Fe^{2+} and Co^{2+} ions have usually been introduced for homogeneous activation of persulfate (Chan & Chu 2009; Xu & Li 2010). Nevertheless, the catalytic activity of persulfate anions activated with homogeneous Fe^{2+}/Co^{2+} ions is significantly dependent on solution pH, the activator can not be recovered and reused, and Co^{2+} ions have potential ecotoxicity (Bolobajev et al. 2015). In addition, an excess of Fe^{2+} ions is likely to capture SO$_4^{-\bullet}$ in the Fe^{2+}/persulfate system (Equations (1) and (2)) (Zhu et al. 2013):

$$Fe^{2+} + S_2O_8^{2-} \rightarrow Fe^{3+} + SO_4^{2-} + SO_4^{-\bullet} \tag{1}$$

$$Fe^{2+} + SO_4^{-\bullet} \rightarrow Fe^{3+} + SO_4^{2-} \tag{2}$$

To overcome these limitations, solid reagents of iron and cobalt were used to activate persulfate (Equations (3) and (4)) (Yang et al. 2008; Drzewicz et al. 2012; Chen

et al. 2013; Ghauch et al. 2013; Joo 2014; Lee et al. 2014):

$$Fe^0 + 2S_2O_8^{2-} \rightarrow Fe^{2+} + 2SO_4^{2-} + 2SO_4^{-\bullet} \tag{3}$$

$$H_2O + SO_4^{-\bullet} \rightarrow SO_4^{2-} + OH^{\bullet} + H^+ \tag{4}$$

Fe$_3$O$_4$ magnetic nanoparticles (Fe$_3$O$_4$ MNPs) have been used as a suitable heterogeneous catalyst for activating persulfate due to the relatively wide availability and specific structural, easy separation/reuse and environmental friendliness (Yan et al. 2011; Ruan et al. 2015; Zhao et al. 2015). However, Fe$_3$O$_4$ MNPs-based persulfate oxidation is limited by the relatively low catalytic activity, low utilization efficiency of oxidants, and incomplete degradation of organic compounds. Recently, some scholars reported that the stability, dispersibility and catalytic efficiency of Fe$_3$O$_4$ MNPs to persulfate or H$_2$O$_2$ could be improved by modifying their surface with polymers such as poly(3,4-ethylene-dioxythiophene) (Shin et al. 2008), humic acid (Niu et al. 2011), and polyhydroquinone (Leng et al. 2013).

As a monolayer of carbon atoms with a tight packing of honeycomb lattice, graphene has attracted immense research interest in nanotechnology in recent years (Geim & Novoselov 2007). Graphene can increase the charge transfer rate of electrons and the surface-adsorbed amount of chemical molecules through π–π interaction. As a result of its unique physical and chemical properties, graphene oxide (GO) has also been used for adsorbing dye from wastewater discharged from the textiles, printing, and tanning industries (Bradder et al. 2010). More recently, Fe$_3$O$_4$/GO and Fe$_3$O$_4$/graphene composites have sparked much interest in promoting transfer and adsorption properties (Wang et al. 2012; Yao et al. 2012). Nevertheless, to our knowledge, there has been no study of the Fe$_3$O$_4$/graphene composites for activating persulfate so far.

In this study, Fe$_3$O$_4$ MNPs were embedded onto graphene to act as an activator for persulfate generating SO$_4^{-\bullet}$ radicals to oxidize organic target pollutants. Methylene blue (MB) was chosen as the typical dye pollutant. The present work aimed at providing insight into the activating ability and feasibility of Fe$_3$O$_4$/graphene to enhance the decomposition of persulfate and then degrade MB.

MATERIALS AND METHODS

Chemicals

Natural graphite powder was purchased from Qingdao Chenyang Graphite Company, China. MB, FeCl$_3$·6H$_2$O, NaOH and K$_2$S$_2$O$_8$ were purchased from Beijing Chemical Reagent Company (Beijing, China). All other chemicals were of analytical grade and used without further purification. Ultra-pure H$_2$O (>18 MΩ/cm) was used in the experiments.

Preparation of GO

GO was prepared from graphite powder by using a modified Hummers method as described by Wang et al. (2012). In brief, graphite powder (10 g) and NaNO$_3$ (7.5 g) was added with stirring into concentrated H$_2$SO$_4$ (98%, 300 mL) solution in which KMnO$_4$ (40 g) was completely dissolved. After 3 days of vigorous stirring at room temperature, the mixture was added into 1 L of 1% H$_2$O$_2$ solution. Then, the mixture was filtered and washed with deionized water until the pH of the filtrate became neutral. To remove the residual salts and acids, the resulting black paste was subjected to dialysis for 1 week by re-dispersing in deionized water, and then the brown suspension was dried at 40 °C under vacuum. GO was obtained as a gray powder.

Preparation of Fe$_3$O$_4$/graphene

The Fe$_3$O$_4$/graphene nanocomposite was prepared by the solvothermal method (Ai et al. 2011). Typically, a certain amount of the as-prepared GO was completely dispersed in 70 mL ethylene glycol and the mixture was ultrasonicated for 3 h. Then, 1.4 g FeCl$_3$·6H$_2$O and 2.8 g sodium acetate were added into the above mixture. After 30 min of stirring at room temperature, the mixture was transferred into a Teflon stainless-steel autoclave and reacted at 200 °C for 6 h in an oven. Afterwards, the autoclave was taken out of the oven and cooled to room temperature. The obtained Fe$_3$O$_4$/graphene nanocomposite was thoroughly washed sequentially with ultrapure water and ethanol and vacuum-dried at 60 °C. The Fe$_3$O$_4$/graphene composites

with different mass ratios of Fe_3O_4 to GO (1:0.5, 1:1, 1:2, 1:3, 1:5) were synthesized by varying the amount of GO.

Characterization

X-ray powder diffraction (XRD) measurements were carried out with a Bruker D8 advance diffractometer (Bruker, Germany) with Cu Kα radiation from 5 to 70 $^\circ$ at a rate of 0.2 $^\circ$/s. Fourier transform infrared (FT-IR) spectra were obtained by the KBr method with a JIR-6500W FT-IR spectrometer (Nihon Denshi, Tokyo, Japan).

Performance study of the Fe₃O₄/graphene sample

The catalytic degradation experiments of MB were conducted in 250 mL conical flasks sealed with Teflon-lined screw caps under mechanical stirring at various temperatures. In a typical run, 5–25 mg of Fe_3O_4/graphene was added to the flasks containing 100 mL MB solution, followed by 20 min of stirring to reach the adsorption–desorption equilibrium. Then, the MB concentration was measured and taken as the initial concentration. Prior to each experiment, Fe_3O_4/graphene was sonicated for 10 min to obtain well-suspended particles. The reaction was initiated immediately by adding 13.5–81 mg $K_2S_2O_8$. To optimize the treatment efficiency of MB degradation by $K_2S_2O_8$ using Fe_3O_4/graphene as the activator, five activator dosage gradients (50, 100, 150, 200 and 250 mg/L), six oxidant dosage gradients (0.5, 1.0, 1.5, 2.0, 2.5 and 3.0 mM), five pH gradients (pH 4.0, 5.0, 6.0, 7.0 and 8.0), and five temperature gradients (15, 25, 35, 45 and 55 °C) were chosen to study their effects on the degradation efficiency. The solution pH was adjusted by using NaOH (1.0 M) or H_2SO_4 (1.0 M) solution. At selected time intervals, 2 mL of samples were collected from each replicate flask, and immediately filtered through 0.22 μm membrane. After filtration, 0.2 mL of 0.2 mM Na_2SO_3 solution was added into the filtrate to quench any residual sulfate radicals and hydroxyl radicals (Tan *et al.* 2014).

The used activator was collected by a permanent magnet, rinsed with Milli-Q water several times, dried at 80 °C for 12 h, and then used for initiating the second treatment in the same reaction system. The recycled activator would be reused for at least three other cycles.

Analytical methods

The concentrations of MB in the solution were determined using the spectrophotometeric method at 664 nm. The amount of total iron (Fe^{2+} plus Fe^{3+}) leaching from the activator into reaction solutions was monitored by atomic absorption spectroscopy (model Z-2000; Hitachi, Tokyo, Japan). In this study, all oxidation tests were performed in triplicate, and results represented the means of three parallel experiments.

RESULTS AND DISCUSSION

XRD analysis

The phase of the Fe_3O_4/graphene composite with 1:2 Fe_3O_4/GO mass ratio was investigated by XRD, as shown in Figure 1(a). All the diffraction peaks are indexed to the inverse cubic spinel structure of Fe_3O_4 (JCPDS card no. 82-1533). No peak shift is observed when GO was introduced into the Fe_3O_4 MNPs, indicating that the formation of the composites with the present Fe_3O_4/GO mass ratio has a negligible effect on the crystal phase of Fe_3O_4 MNPs. The peaks at 2θ values at 30.0, 35.3, 43.2, 53.4, 57.1, 62.5 and 74.2 $^\circ$ can be indexed to (220), (311), (400), (422), (511), (440), and (533) inverse cubic spinel structure of Fe_3O_4, respectively. The strong and sharp diffraction peaks demonstrated that the synthesized product was well crystallized. Similarly to the previous TiO_2/graphene composite using GO as the precursor of graphene (Zhang *et al.* 2010), no typical diffraction peaks of GO were detected (Figure 1(a)), which can be explained by (1) the reduction of GO to graphene by ethylene glycol and (2) the destroyed regular stack of GO by the intercalation of Fe_3O_4.

FT-IR analysis

Figure 1(b) shows the FT-IR spectra of GO and Fe_3O_4/graphene. Fe_3O_4/graphene and GO both show the O–H stretching vibration adsorption peak at 3,430 cm^{-1}. The bands at 1,628 and 1,632 cm^{-1} are associated with
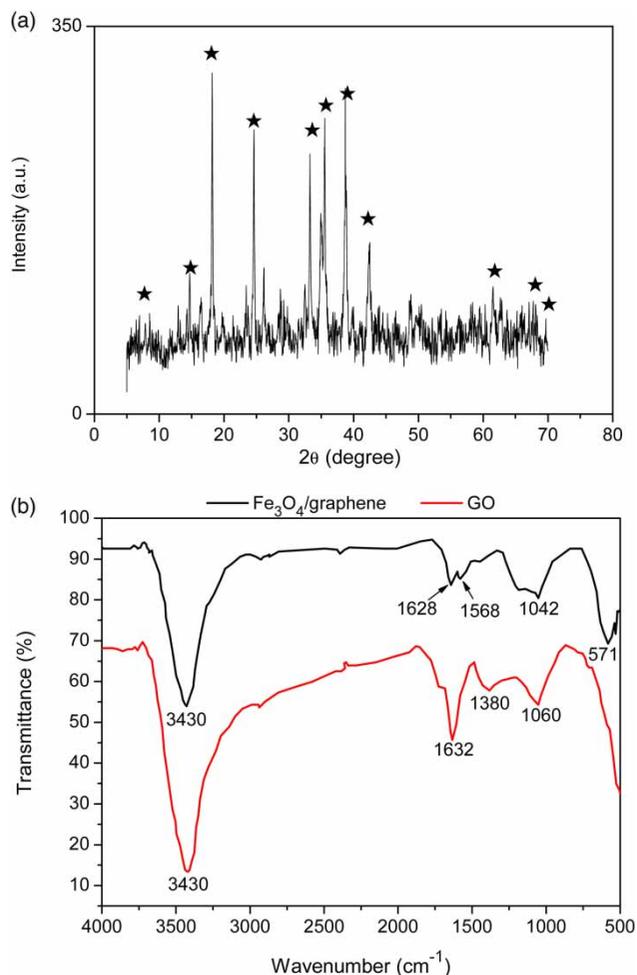
Figure 1 │ XRD pattern (a) and FT-IR spectra (b) of the obtained Fe$_3$O$_4$/graphene. The Fe$_3$O$_4$/graphene composite was synthesized with a 1:2 Fe$_3$O$_4$/GO weight ratio.

Figure 2 │ Degradation efficiency of MB by Fe$_3$O$_4$ and Fe$_3$O$_4$/graphene prepared with different mass ratios of Fe$_3$O$_4$ to GO as a function of time. Reaction conditions: [Fe$_3$O$_4$/graphene (or Fe$_3$O$_4$)]$_0$ = 150 mg/L, [K$_2$S$_2$O$_8$]$_0$ = 2.0 mM, [MB]$_0$ = 0.05 mM, temperature 25 °C, pH 6.0.

Effect of Fe$_3$O$_4$/GO mass ratio on degradation effectiveness

Figure 2 shows the time course of chemical degradation of MB at an initial concentration of 0.05 mM by Fe$_3$O$_4$ and Fe$_3$O$_4$/graphene prepared with various Fe$_3$O$_4$/GO mass ratios. From Figure 2, it can be seen that the Fe$_3$O$_4$/GO mass ratio had an obvious impact on the degradation efficiency of MB. The free Fe$_3$O$_4$ exhibited lower catalytic activity, giving a 72.4% degradation of MB after 120 min. The catalytic activity of Fe$_3$O$_4$/graphene could be efficiently improved by graphene loading (Figure 2). Specifically, the degradation ratio of MB increased with the increase in the Fe$_3$O$_4$/GO mass ratio up to 1:2 in the Fe$_3$O$_4$/graphene samples. This is attributed to the enhanced adsorption capacity of Fe$_3$O$_4$/graphene nanocomposite for MB molecules and the increased rate of electron transfer in solution by graphene loading (Geim & Novoselov 2007; Ai et al. 2011; Chang et al. 2012; Yao et al. 2012; Zhou et al. 2014). Nearly a 100% degradation of MB could be obtained within 120 min of using Fe$_3$O$_4$/graphene with a 1:2 Fe$_3$O$_4$/GO mass ratio (Figure 2). However, when the Fe$_3$O$_4$/GO mass ratio was further increased from 1:2 to 1:5, MB degradation efficiency decreased. This is because the number of Fe$_3$O$_4$ active sites decreased with increasing the Fe$_3$O$_4$/GO mass ratio, leading to fewer reaction sites for catalytic degradation. Therefore, the suitable Fe$_3$O$_4$/GO mass ratio for MB

stretching of the C = O bond of carboxyl groups. The band at 1,380 cm^{-1} is the C = O stretching vibration peak of carboxyl and carbonyl. The band at 1,060 cm^{-1} is ascribed to the C–O stretching vibration of the epoxy group and alkoxy (Chandra et al. 2010). The band at 571 cm^{-1}, which only presents in the FT-IR spectrum of Fe$_3$O$_4$/graphene, can be ascribed to lattice absorption of iron oxide. Additionally, a new band is observed at 1,568 cm^{-1} for Fe$_3$O$_4$/graphene, which is attributed to the asymmetric vibration of COO$^-$. This is the evidence for plenty of COO$^-$ coordinated with ferric ion (Ge et al. 2007). In comparison with GO, Fe$_3$O$_4$/graphene shows a dramatic decrease in the intensity of adsorption bands of oxygen-containing functional groups, indicating that GO has been substantially reduced.
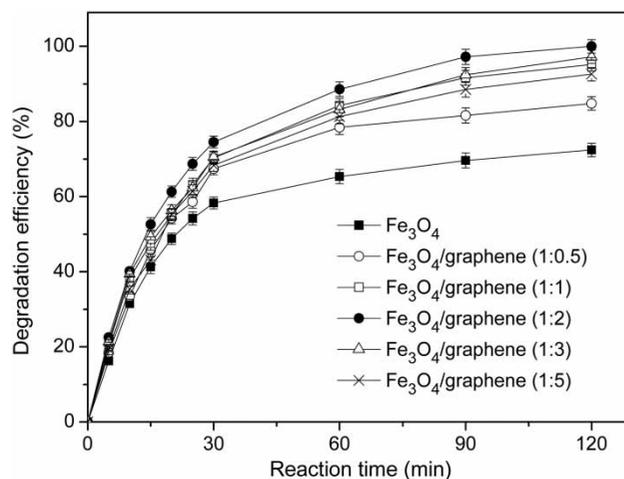
degradation by K$_2$S$_2$O$_8$ is recommended as 1:2 and further experiments were performed using this type of Fe$_3$O$_4$/graphene. In this study, MB removal by Fe$_3$O$_4$/GO adsorption was about 0.7% of its initial concentration, which was negligible relative to the removal efficiency of MB through oxidation.

Effect of Fe$_3$O$_4$/graphene dosage on degradation effectiveness

To check the catalytic activity of Fe$_3$O$_4$/graphene composite on persulfate for the degradation of MB, a set of experiments was conducted for 120 min with the Fe$_3$O$_4$/graphene dosage ranging from 50 to 250 mg/L. The experiments were run with an initial MB concentration of 0.05 mM, fixed persulfate concentration of 1.5 mM, pH 6.0 and at 25 °C.

Figure 3 illustrates the degradation efficiency of MB with time at different activator dosages in solution. The control experiment only showed 9.3% loss of MB in the absence of Fe$_3$O$_4$/graphene, suggesting a low oxidation capacity of persulfate without activator. As expected, an enhancement of MB degradation is observed by increasing Fe$_3$O$_4$/graphene from 50 to 150 mg/L. A 40% degradation of MB is reached within 30 min at 50 mg/L Fe$_3$O$_4$/graphene, whereas the same degradation could be reached within 20 and 10 min at Fe$_3$O$_4$/graphene dosages of 100 mg/L and
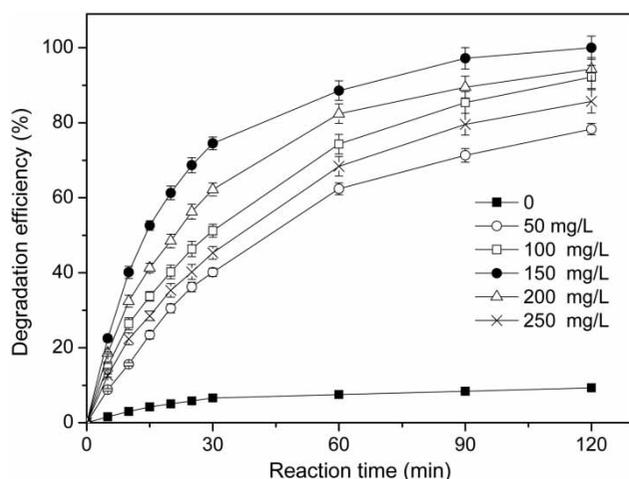

Figure 3 │ Effect of Fe$_3$O$_4$/graphene dosage on MB degradation as a function of time. Reaction conditions: [K$_2$S$_2$O$_8$]$_0$ = 1.5 mM, [MB]$_0$ = 0.05 mM, temperature 25 °C, pH 6.0. The used Fe$_3$O$_4$/graphene was prepared with a 1:2 Fe$_3$O$_4$/GO mass ratio.

150 mg/L, respectively. The fact is evidently attributed to the increased concentration of active sites of Fe$_3$O$_4$ for reaction with persulfate, which would generate more reactive SO$_4^{\cdot-}$ (Equation (1)) (Ding et al. 2012; Tan et al. 2014). Thus, increasing the dosage of Fe$_3$O$_4$/graphene benefited the degradation of MB. However, it is found that as the dosage of Fe$_3$O$_4$/graphene was increased from 150 to 250 mg/L, MB degradation decreased (Figure 3). This can be explained by (1) increased quenching of SO$_4^{\cdot-}$ species due to the combination between SO$_4^{\cdot-}$ species themselves caused by the excess of the activator (Yan et al. 2011), and (2) increased quenching of SO$_4^{\cdot-}$ with Fe^{2+} at high dosage of the activator through Equation (2). Thereupon, MB degradation decreased when the Fe$_3$O$_4$/graphene was added further beyond about 150 mg/L. When a moderate dosage of Fe$_3$O$_4$/graphene was added, there existed a competition between SO$_4^{\cdot-}$ quenching and reacting with MB, showing slower increment of MB degradation with the increase of Fe$_3$O$_4$/graphene addition.

Effect of persulfate concentration on degradation effectiveness

Oxidant concentration has an important influence on the treatment process efficiency and operational costs. To elucidate the role of persulfate concentration on the degradation of MB, a set of experiments were conducted for 120 min with the persulfate concentration ranging from 0.5 to 3.0 mM. The experiments were run with an initial MB concentration of 0.05 mM, fixed Fe$_3$O$_4$/graphene dosage of 150 mg/L, pH 6.0 and at 25 °C.

As shown in Figure 4, a lower degradation of MB is observed in the presence of 0.5 mM persulfate. Under the conditions, the mole ratio of persulfate to MB was 10. The incomplete degradation of MB is due to lack of a sufficient SO$_4^{\cdot-}$ amount. When the persulfate concentration was raised to 2.0 mM, the degradation efficiency increased, as more active radicals could be generated under higher concentrations of persulfate. Within 120 min, the degradation efficiency of MB had reached 100% with 2.0 mM persulfate. Hence, a further increase in the persulfate concentration to 3.0 mM did not improve the degradation efficiency but only enhanced the initial degradation rate. For instance, 100% degradation of MB is obtained within 90 and 60 min at the
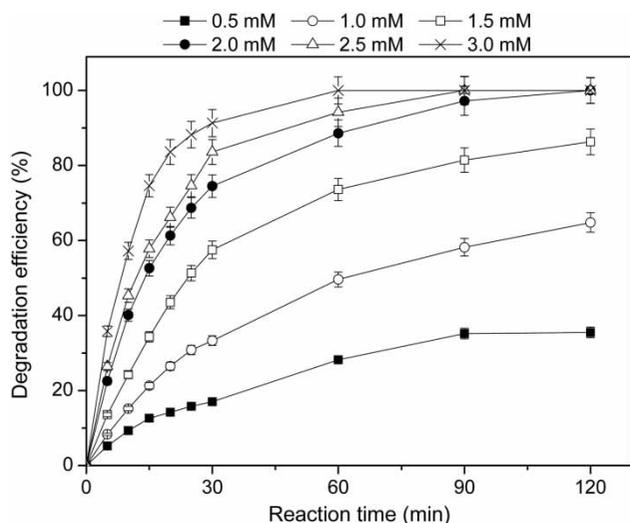
Figure 4 │ Effect of persulfate concentration on MB degradation as a function of time. Reaction conditions: $[Fe_3O_4/graphene]_0 = 150$ mg/L, $[MB]_0 = 0.05$ mM, temperature 25 °C, pH 6.0. The used Fe_3O_4/graphene was prepared with a 1:2 Fe_3O_4/GO mass ratio.

Figure 5 │ Effect of initial solution pH on MB degradation as a function of time. Reaction conditions: $[Fe_3O_4/graphene]_0 = 150$ mg/L, $[K_2S_2O_8]_0 = 1.5$ mM, $[MB]_0 = 0.05$ mM, temperature 25 °C. The used Fe_3O_4/graphene was prepared with a 1:2 Fe_3O_4/GO mass ratio.

persulfate concentration of 2.5 mM and 3.0 mM, respectively. This may be due to the fact that the reaction rate is limited by radical generation under low concentrations of persulfate, but by radical attraction to the dye under high persulfate concentrations.

Effect of initial solution pH on degradation effectiveness

The influence of initial solution pH was investigated on the MB degradation in the system of 0.05 mM MB + 1.5 mM $K_2S_2O_8$ + 150 mg/L Fe_3O_4/graphene.

Figure 5 demonstrates that the degradation rate decreased as pH rose from 4.0 to 8.0. In pH 4.0, the dye can be completely degraded within 30 min. At an initial pH of 6.0, the degradation rate became much slower; however, a removal of 100% could still be obtained within 120 min, implying that the activator still exhibited a good catalytic activity under near-neutral conditions. This is of importance for wastewater treatment because it is unnecessary to pre-adjust wastewater pH. When the reaction was conducted in alkaline solution (pH 8.0), a rapid degradation of MB occurred during the first 10 min followed by a substantial decrease with a final removal of about 54% after 120 min.

Similar results were also reported in sulfamonomethox-ine degradation by Fe_3O_4 activated persulfate system (Yan
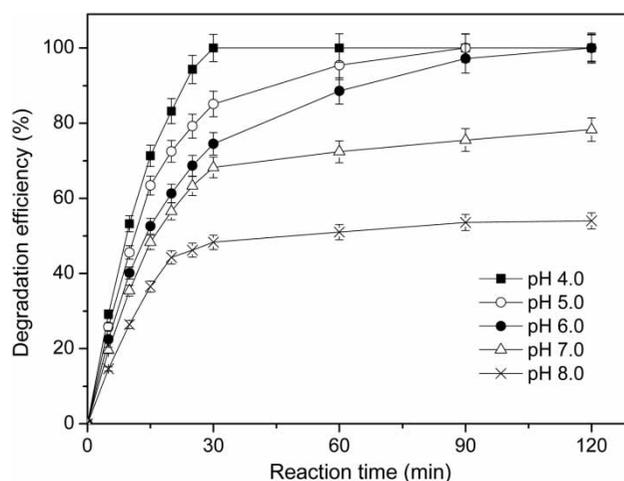
et al. 2011). In aqueous solution, MB and persulfate are presented as negative ions, thus increasing solution pH would increase the amount of negative surface charge on the activator. This would inhibit the static interactions between Fe_3O_4/graphene and MB or persulfate, and consequently result in a slower rate of reactive species production and dye degradation. Moreover, self-dissociation of persulfate mainly through non-radical pathways increases with an increment in solution pH, which would additionally reduce the degradation efficiency of the target pollutants (Rastogi et al. 2009).

Effect of temperature on degradation effectiveness

It is known that the oxidation capability of persulfate is moderate at room temperature, and the formation rate of $SO_4^{\cdot-}$ is pronounced at higher temperatures due to the increased thermal decomposition of persulfate (Kolthoff & Miller 1951). To investigate the influence of temperature on persulfate oxidation of aqueous MB solution (0.05 mM), a series of experiments were conducted at an initial persulfate concentration of 1.5 mM, an initial Fe_3O_4/graphene dosage of 150 mg/L, and an initial pH of 6.0 in the temperature range of 15–55 °C.

As shown in Figure 6, the degradation rate of MB was significantly enhanced by raising the temperature. Complete degradation of MB was observed in 120, 90, 60 and 20 min when the reaction was carried out at 25 °C, 35 °C, 45 °C and
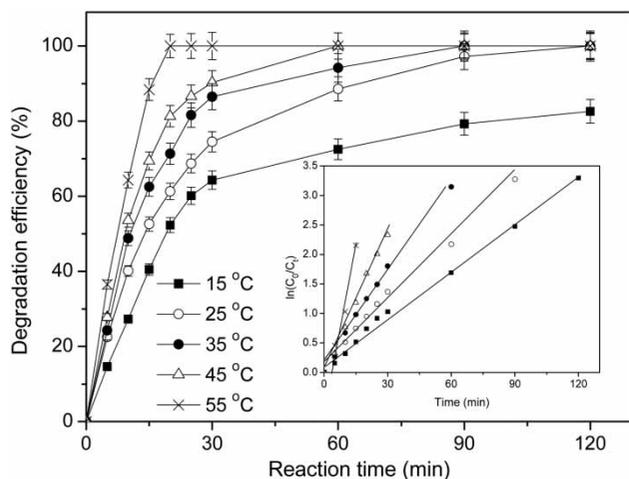
Figure 6 | Effect of temperature on MB degradation as a function of time. Reaction conditions: $[Fe_3O_4/graphene]_0 = 150$ mg/L, $[K_2S_2O_8]_0 = 1.5$ mM, $[MB]_0 = 0.05$ mM, pH 6.0. The used Fe_3O_4/graphene was prepared with a 1:2 Fe_3O_4/GO weight ratio.

55 °C, respectively, whereas only 82.6% MB was removed at a temperature of 15 °C after 120 min. These results suggest that persulfate could be converted to SO_4^- radicals by thermal energy resulting in a considerable enhancement in the reaction rates with increasing temperature.

In general, chemical degradation of pollutants by persulfate oxidation in aqueous phase is assumed to be a pseudo-first-order reaction (Tan *et al.* 2014; Zhao *et al.* 2015). The pseudo-first-order kinetics can be expressed as Equation (5):

$$\ln(C_0/C_t) = kt + y \qquad (5)$$

where y is a constant, t is reaction time (min), k is the apparent rate constant (min^{-1}), C_0 and C_t are MB concentrations (mM) at $t = 0$ and $t = t$, respectively. As shown in the insert of Figure 6, MB abatement via persulfate oxidation followed pseudo-first order kinetics with respect to reaction time ($R^2 \geq 0.98$). The degradation rate of k was increased with the enhancement of temperature from 15 to 55 °C ($k = 0.024$ min^{-1}, 0.031 min^{-1}, 0.049 min^{-1}, 0.081 min^{-1} and 0.141 min^{-1}, respectively, which is in agreement with the studies of others (Tan *et al.* 2014; Zhao *et al.* 2015).

Stability and reusability of Fe₃O₄/graphene

To evaluate and compare the reusability of the activators, the prepared Fe_3O_4/graphene and Fe_3O_4 nanocomposites were repeatedly used to activate persulfate five times. After each run, the activators were collected using a magnet, rinsed with distilled water, and then recycled for the next batch of MB degradation treatment. Figure 7(a) shows that when the recycle number of the activators increased, the degradation efficiency of MB gradually decreased in the case of Fe_3O_4/graphene, but decreased remarkably in the case of Fe_3O_4. After the fifth usage, the removal efficiency of MB was 64.6% for Fe_3O_4/graphene but was only 17.3% for Fe_3O_4. This indicates that the Fe_3O_4/graphene has a high reusability because of graphene loading. It has been found that most of the catalytic activity of free Fe_3O_4 could be lost after reuse several times (Tan *et al.* 2014; Zhao *et al.* 2015). The decrease in the removal efficiency
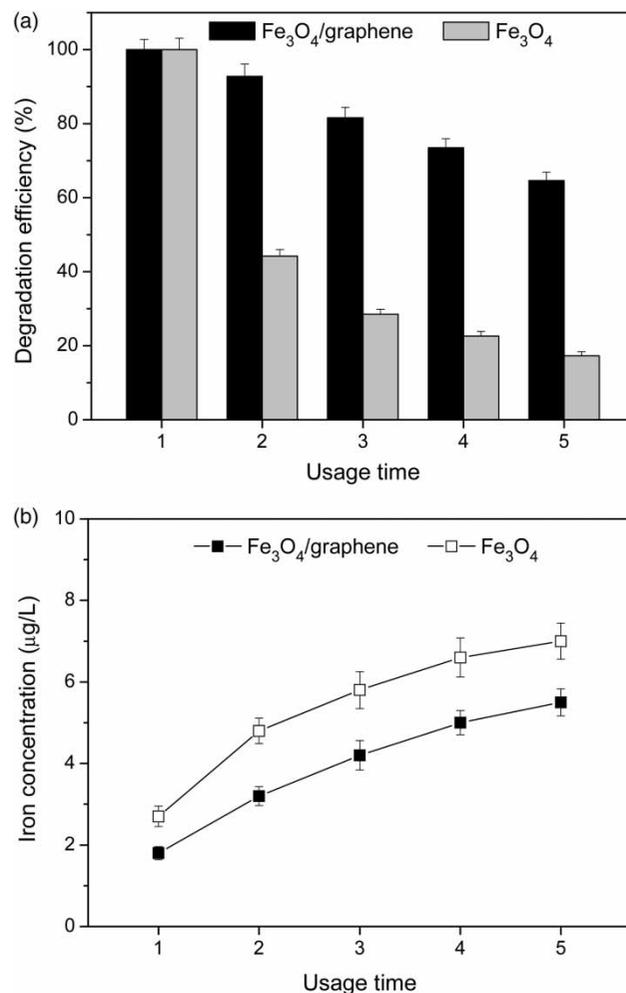

Figure 7 | Effect of usage number of Fe_3O_4 and Fe_3O_4/graphene on MB degradation (a) and iron leaching (b). Reaction conditions: $[Fe_3O_4/graphene]_0 = 150$ mg/L, $[Fe_3O_4]_0 = 50$ mg/L, $[K_2S_2O_8]_0 = 1.5$ mM, $[MB]_0 = 0.05$ mM, pH 6.0, temperature 25 °C, reaction time 120 min. The used Fe_3O_4/graphene was prepared with a 1:2 Fe_3O_4/GO weight ratio.

can be explained by (i) the conversion of the ≡Fe^{2+} to ≡Fe^{3+} on the surface of Fe_3O_4 (Zhao *et al.* 2015) and (ii) the reduction of the surface area of materials due to the agglomeration of activator particles during the reaction (Tan *et al.* 2014).

To evaluate the stability of the Fe_3O_4/graphene activator, the leaching of Fe^{2+} and Fe^{3+} was determined over time during persulfate oxidation of MB. Under the experimental conditions, Fe^{2+} ions leached were rapidly oxidized to Fe^{3+} ions by the radicals, thus only Fe^{3+} ions were detected and presented. As shown in Figure 7(b), as the cycle time increased, the concentration of Fe^{3+} leached increased gradually but was always below the legal limits of USA and China (300 µg/L). Moreover, the concentration of Fe^{3+} was lower in the case of Fe_3O_4/graphene than in the case of Fe_3O_4. This suggests that the Fe_3O_4/graphene activator was stable during the catalytic reactions.

CONCLUSIONS

In the present study, Fe_3O_4/graphene nanocomposite was prepared and characterized by XRD and FT-IR. The effects of different conditions on the degradation of MB by Fe_3O_4/graphene activated persulfate were investigated. Results show that Fe_3O_4/graphene could effectively catalyze persulfate to degrade MB. Within 120 min of reaction time, almost 100% of 0.05 mM MB was removed at an initial persulfate concentration of 1.5 mM in the presence of 150 mg/L of Fe_3O_4/graphene at pH = 6.0 and 25 °C. Under the experimental conditions, the reactions followed the pseudo-first-order kinetics model. Fe_3O_4/graphene exhibited good stability and reusability, and it can be reused several times by separation from solution with employment of an external magnet. The Fe_3O_4/graphene showed better catalytic performance and excellent reusability compared to free Fe_3O_4. During the reaction, the activator was stable without significant leaching of iron into water.

REFERENCES

Ai, L., Zhang, C. & Chen, Z. 2011 Removal of methylene blue from aqueous solution by a solvothermal-synthesized graphene/magnetite composite. *J. Hazard. Mater.* **192**, 1515–1524.

Anipsitakis, G. P. & Dionysiou, D. D. 2004 Radical generation by the interaction of transition metals with common oxidants. *Environ. Sci. Technol.* **38**, 3705–3712.

Bolobajev, J., Öncü, N. B., Viisimaa, M., Trapido, M., Balcıoğlu, I. & Goi, A. 2015 Column experiment on activation aids and biosurfactant application to the persulphate treatment of chlorophene-contaminated soil. *Environ. Technol.* **36**, 348–357.

Bradder, P., Ling, S. K., Wang, S. & Liu, S. 2010 Dye adsorption on layered graphite oxide. *J. Chem. Eng. Data* **56**, 138–141.

Chan, K. H. & Chu, W. 2009 Degradation of atrazine by cobalt-mediated activation of peroxymonosulfate: different cobalt counteranions in homogenous process and cobalt oxide catalysts in photolytic heterogeneous process. *Water Res.* **43**, 2513–2521.

Chandra, V., Park, J., Chun, Y., Lee, J. W., Hwang, I. C. & Kim, K. S. 2010 Water-dispersible magnetite-reduced graphene oxide composites for arsenic removal. *ACS Nano* **4**, 3979–3986.

Chang, Y. P., Ren, C. L., Qu, J. C. & Chen, X. G. 2012 Preparation and characterization of Fe_3O_4/graphene nanocomposite and investigation of its adsorption performance for aniline and p-chloroaniline. *Appl. Surf. Sci.* **261**, 504–509.

Chen, S. S., Hsu, H. T., Tsui, H. J. & Chang, Y. M. 2013 Removal of nonionic surfactant from electroplating wastewater by fluidized zerovalent iron with two oxidants (H_2O_2/$Na_2S_2O_8$). *Desalin. Water Treat.* **251**, 1678–1684.

Ding, Y., Zhu, L., Wang, N. & Tang, H. 2012 Sulfate radicals induced degradation of tetrabromobisphenol a with nanoscaled magnetic $CuFe_2O_4$ as a heterogeneous catalyst of peroxymonosulfate. *Appl. Catal. B* **129**, 153–162.

Drzewicz, P., Perez-Estrada, L., Alpatova, A., Martin, J. W. & Gamal El-Din, M. 2012 Impact of peroxydisulfate in the presence of zero valent iron on the oxidation of cyclohexanoic acid and naphthenic acids from oil sands process-affected water. *Environ. Sci. Technol.* **46**, 8984–8991.

Ge, J., Hu, Y., Biasini, M., Beyermann, W. P. & Yin, Y. 2007 Superparamagnetic magnetite colloidal nanocrystal clusters. *Angew. Chem. Int. Edit.* **46**, 4342–4345.

Geim, A. K. & Novoselov, K. S. 2007 The rise of graphene. *Nature Mater.* **6**, 183–191.

Ghauch, A., Ayoub, G. & Naim, S. 2013 Degradation of sulfamethoxazole by persulfate assisted micrometric Fe^0 in aqueous solution. *Chem. Eng. J.* **228**, 1168–1181.

Joo, S. H. 2014 Advanced treatment of reverse osmosis concentrate by integrated activated carbon and iron-activated persulfate oxidation. *Water Air Soil Pollut.* **225**, 2076.

Kolthoff, I. M. & Miller, I. K. 1951 The chemistry of persulfate. I. The kinetics and mechanism of the decomposition of the persulfate ion in aqueous medium. *J. Am. Chem. Soc.* **73**, 3055–3059.

Lee, H., Yoo, H. Y., Choi, J., Nam, I. H., Lee, S., Lee, S., Kim, J. H., Lee, C. & Lee, J. 2014 Oxidizing capacity of periodate activated with iron-based bimetallic nanoparticles. *Environ. Sci. Technol.* **48**, 8086–8093.

Leng, Y., Guo, W., Shi, X., Li, Y. & Xing, L. 2013 Polyhydroquinone-coated Fe_3O_4 nanocatalyst for degradation of rhodamine B based on sulfate radicals. *Ind. Eng. Chem. Res.* **52**, 13607–13612.

Liu, C. S., Shih, K., Sun, C. X. & Wang, F. 2012 Oxidative degradation of propachlor by ferrous and copper ion activated persulfate. *Sci. Total Environ.* **416**, 507–512.

Niu, H. Y., Zhang, D., Zhang, S. X., Zhang, X. L., Meng, Z. F. & Cai, Y. Q. 2011 Humic acid coated Fe_3O_4 magnetic nanoparticles as highly efficient Fenton-like catalyst for complete mineralization of sulfathiazole. *J. Hazard. Mater.* **190**, 559–565.

Rastogi, A., Al-Abed, S. R. & Dionysiou, D. D. 2009 Sulfate radical-based ferrous–peroxymonosulfate oxidative system for PCBs degradation in aqueous and sediment systems. *Appl. Catal. B* **85**, 171–179.

Ruan, X., Gu, X., Lu, S., Qiu, Z. & Sui, Q. 2015 Trichloroethylene degradation by persulfate with magnetite as heterogeneous activator in aqueous solution. *Environ. Technol.* **36**, 1389–1397.

Shin, S., Yoon, H. & Jang, J. 2008 Polymer-encapsulated iron oxide nanoparticles as highly efficient Fenton catalysts. *Catal. Commun.* **10**, 178–182.

Tan, C., Gao, N., Deng, Y., Deng, J., Zhou, S., Li, J. & Xin, X. 2014 Radical induced degradation of acetaminophen with Fe_3O_4 magnetic nanoparticles as heterogeneous activator of peroxymonosulfate. *J. Hazard. Mater.* **276**, 452–460.

Tsitonaki, A., Petri, B., Crimi, M., Mosbæk, H., Siegrist, R. L. & Bjerg, P. L. 2010 *In situ* chemical oxidation of contaminated soil and groundwater using persulfate: a review. *Crit. Rev. Environ. Sci. Technol.* **40**, 55–91.

Wang, J., Tang, B., Tsuzuki, T., Liu, Q., Hou, X. & Sun, L. 2012 Synthesis, characterization and adsorption properties of superparamagnetic polystyrene/Fe_3O_4/graphene oxide. *Chem. Eng. J.* **204**, 258–263.

Xu, X. R. & Li, X. Z. 2010 Degradation of azo dye orange G in aqueous solutions by persulfate with ferrous ion. *Sep. Purif. Technol.* **72**, 105–111.

Yan, J. C., Lei, M., Zhu, L. H., Anjum, M. N., Zou, J. & Tang, H. Q. 2011 Degradation of sulfamonomethoxine with Fe_3O_4 magnetic nanoparticles as heterogeneous activator of persulfate. *J. Hazard. Mater.* **186**, 1398–1404.

Yang, Q. J., Choi, H., Chen, Y. J. & Dionysiou, D. D. 2008 Heterogeneous activation of peroxymonosulfate by supported cobalt catalysts for the degradation of 2,4-dichlorophenol in water: the effect of support, cobalt precursor, and UV radiation. *Appl. Catal. B* **77**, 300–307.

Yao, Y., Miao, S., Liu, S., Ma, L. P., Sun, H. & Wang, S. 2012 Synthesis, characterization, and adsorption properties of magnetic Fe_3O_4:graphene nanocomposite. *Chem. Eng. J.* **184**, 326–332.

Zhang, Y., Tang, Z. R., Fu, X. & Xu, Y. J. 2010 TiO_2-graphene nanocomposites for gas-phase photocatalytic degradation of volatile aromatic pollutant: is TiO_2- graphene truly different from other TiO_2-carbon composite materials? *ACS Nano* **4**, 7303–7314.

Zhang, M., Chen, X., Zhou, H., Murugananthan, M. & Zhang, Y. 2015 Degradation of p-nitrophenol by heat and metal ions co-activated persulfate. *Chem. Eng. J.* **264**, 39–47.

Zhao, Y. S., Sun, C., Sun, J. Q. & Zhou, R. 2015 Kinetic modeling and efficiency of sulfate radical-based oxidation to remove p-nitroaniline from wastewater by persulfate/Fe_3O_4 nanoparticles process. *Sep. Purif. Technol.* **142**, 182–188.

Zhou, C., Zhang, W., Wang, H., Li, H., Zhou, J., Wang, S., Liu, J., Luo, J., Zou, B. & Zhou, J. 2014 Preparation of Fe_3O_4-embedded graphene oxide for removal of methylene blue. *Arab. J. Sci. Eng.* **39**, 6679–6685.

Zhu, L., Ai, Z., Ho, W. & Zhang, L. 2013 Core–shell Fe–Fe_2O_3 nanostructures as effective persulfate activator for degradation of methyl orange. *Sep. Purif. Technol.* **108**, 159–165.